Evidence of a defined spatial arrangement of hyaluronate in the central filament of cartilage proteoglycan aggregates

Matthias MÖRGELIN,*|| Mats PAULSSON,† Dick HEINEGÅRD,* Ueli AEBI‡ and Jürgen ENGEL§

*Department of Medical and Physiological Chemistry, University of Lund, P.O. Box 94, S-22100 Lund, Sweden
†M.E. Müller-Institute for Biomechanics, University of Bern, Postfach 30, CH-3010 Bern, Switzerland
‡M.E. Müller-Institute for High Resolution Electron Microscopy, Biocenter of the University of Basel, Klingelbergstrasse 70, CH-4056 Basel, Switzerland, and §Department of Biophysical Chemistry, Biocenter of the University of Basel, Klingelbergstrasse 70, CH-4056 Basel, Switzerland

Aggregates of proteoglycans from the Swarm rat chondrosarcoma reassembled *in vitro* have been studied by rotary-shadowing electron microscopy, and shown to be similar to native structures that have never been dissociated [Mörgelin, Engel, Heinegård and Paulsson (1992) J. Biol. Chem. **267**, 14275–14284]. A hyaluronate with defined chain length (HA_{short}) has now been prepared by autoclaving high-M_r hyaluronate and fractionation to a narrow size distribution by gel filtration. Proteoglycan monomers, core protein, hyaluronate-binding region and link protein were combined with HA_{short}. Free chains of HA_{short} and reconstituted complexes with proteoglycan, link protein and aggrecan fragments were examined by electron microscopy after rotary shadowing. Length measurements showed that the hyaluronate was condensed to about half of its original length on binding intact aggrecan monomers, any aggrecan fragment or link protein alone. This strongly implies that hyaluronate adopts a defined spatial arrangement within the central filament of the aggregate, probably different from its secondary structure in solution. No differences in length were observed between link-free and link-stabilized aggregates.

INTRODUCTION

Proteoglycans are a polydisperse class of macromolecules which are versatile components of extracellular matrices. They consist of a core protein substituted with one or many characteristic glycosaminoglycan chains as well as N- and O-linked oligosaccharides. The major proteoglycan in hyaline cartilage, aggrecan, is a high-M_r species in which typically some 100 chondroitin sulphate chains, some 30 keratan sulphate chains and about 60 shorter oligosaccharides are linked to an extended core protein. A large proportion of the proteoglycans are present as aggregates formed by the non-covalent interaction between proteoglycan monomers and hyaluronate (Figure 1). The resulting polyanionic supramolecular assemblies have high charge densities and attract large amounts of water, this being crucial for the biomechanical properties of cartilage such as resilience to load (for reviews see [1–4]).

The aggrecan monomers interact specifically with hyaluronate [5]. The binding is through a specialized portion of their core protein, the hyaluronate-binding region [6], to a decasaccharide segment of the hyaluronate chain [9]. This interaction is stabilized by the binding of a small glycoprotein, the link protein [6,8], with affinity for both hyaluronate [9,10] and the hyaluronate-binding region of the aggrecan monomer, leading to the formation of a very stable ternary complex [11]. This model has been extended by a combination of electron microscopy [12–14] and sequence analysis at the protein [15] and cDNA [16–20] level.

Accordingly several structural and functional domains can be distinguished in the M_r-220000 aggrecan core protein [17]. At the N-terminus a pair of globular domains, G1 and G2, are located, interspaced by an extended domain E1 [13]. G1 corresponds to the hyaluronate-binding region [14] and contains loop structures that are homologous both to G2 and the link protein [15,17]. In spite of its sequence homology to G1 the somewhat smaller globular domain G2 does not bind to hyaluronate [14,21]. G2 is followed by the extended strand E2, constituting both the keratan sulphate- and chondroitin sulphate-attachment regions [13]. E2 is terminated by the C-terminal globular domain, G3, showing sequence homology to a class of mammalian lectins [16–20]. The cartilage aggrecan domain structure has recently been reviewed elsewhere [22].

Electron-microscopic characterization of cartilage aggrecan structure was initiated in the 1970s [23,24] using the Kleinschmidt spreading technique originally developed for nucleic acids [25]. This revealed proteoglycan monomers bound along the hyaluronate in aggregates as well as the general organization of side-chain constituents along the core protein [23,26]. When proteoglycans were sprayed on to mica surfaces using the glycerol-spraying/rotary-shadowing technique [27–29], individual domains of the core protein were resolved [12,13]. Furthermore, a continuous central filament with a tight packing of aggrecan monomer G1 domains and link protein along hyaluronate was observed [12,14].

To reveal additional structural details of the central filament consisting of hyaluronate, hyaluronate-binding region G1 and link protein, the present study was undertaken, using the Swarm rat chondrosarcoma as a source of proteoglycan aggregates, monomers and link protein. Novel information on the mode of interaction of the G1 domain and link protein with hyaluronate was obtained in reconstitution experiments with hyaluronate fractionated to narrow and defined length distribution.

MATERIALS AND METHODS

A previous report [30] described some of the reagents and experimental procedures used in the present study including

Abbreviation used: HA_{short}, hyaluronate of defined chain length.
|| To whom correspondence should be addressed.

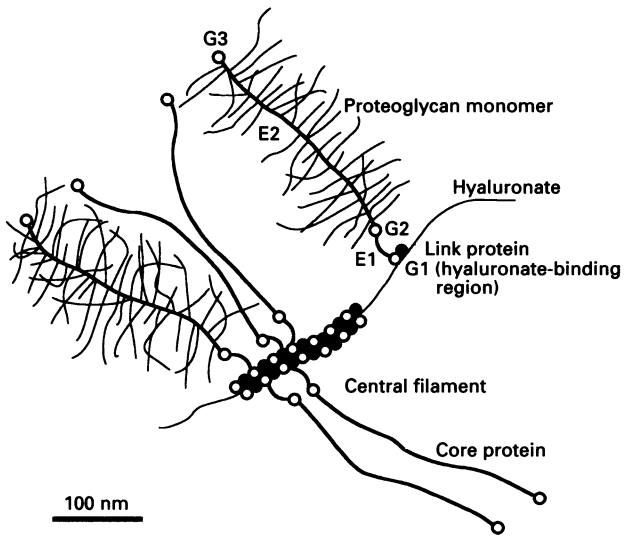

Figure 1 Schematic model of the aggrecan aggregate structure, based on rotary-shadowing electron microscopy

The proteoglycan monomer (aggrecan) binds to hyaluronate by its N-terminal globular core-protein domain G1 (hyaluronate-binding region). The extended domain E1 connects G1 with the globular domain G2 at a spacing of about 25 nm. G2 is followed by the long extended domain E2 (about 280 nm), which is heavily substituted with glycosaminoglycan chains, as indicated for just two of the proteoglycans. E2 is terminated by the C-terminal globular domain G3, which is present in 50–60% of the particles of an average preparation. The binding of G1 to hyaluronate is further stabilized by link protein so that a continuous compact central filament of these three components is formed. The arrangement of G1 and link protein in the central filament is hypothetical.

maintenance of the Swarm rat chondrosarcoma, extraction of tumour tissue and isolation of proteoglycan aggregates, monomers, core protein and link protein either from associative (a-A1) or dissociative extracts (A1). Additional materials and procedures are described below.

Chondroitinase digestion of proteoglycan monomer

Core protein was prepared from rat chondrosarcoma proteoglycan monomers of an A1D1 fraction by digestion with chondroitinase ABC (Sigma) (10 units/g for 6 h at 37 °C) in the presence of ovomucoid (10 μg/ml) as a protease inhibitor in 0.1 M sodium acetate/0.1 M Tris/HCl, pH 7.3. (According to the nomenclature of Heinegård [31] the term A1D1 is used to indicate high-buoyant-density aggrecan monomers prepared from aggregates under dissociative conditions.) Core protein was isolated by chromatography of the digest on Sepharose CL-6B, which was eluted with 0.5 M sodium acetate, pH 7.0. Electron-microscopic inspection revealed traces of remaining hyaluronate–core-protein complexes, which were subsequently removed by chromatography on Sepharose CL-2B, eluted with 0.5 M sodium acetate, pH 7.0.

Preparation of hyaluronate-binding-region fragment G1

Proteoglycan aggregates were prepared by extraction of bovine nasal cartilage with 4 M guanidine hydrochloride (GuHCl), followed by caesium chloride-density-gradient centrifugation under associative conditions (for details and references, see [1]). Purified aggregates (10 mg/ml) were next digested with trypsin (40 μg/ml for 8 h at 37 °C), followed by purification of the resulting hyaluronate-binding-region–link-protein complex by caesium chloride-density-gradient centrifugation and Sepharose CL-2B gel filtration under associative conditions, and, finally, dissociation of the complex in 4 M GuHCl and isolation of the binding region by chromatography on Sephadex G-200 in 4 M GuHCl [6,32].

Reduction and alkylation

Samples of hyaluronate-binding-region fragment (1 mg/ml) were reduced by incubation at 37 °C for 5 h in the presence of 5 mM dithiothreitol/0.05 M Tris/HCl, pH 7.6. The reduced samples were subsequently alkylated by addition of iodoacetic acid to give a final concentration of 15 mM, and incubated in the dark at room temperature for 15 h.

Preparation of narrow-size-distribution hyaluronate (HA_{short})

Purified high-M_r hyaluronate from rooster comb was a gift from Dr. Endre Balazs (Columbia University, New York, NY, U.S.A.). It was dissolved overnight at room temperature in water (10 mg/ml). Aliquots (1 ml) were depolymerized by autoclaving once at 120 °C for 30 min. They were chromatographed on a preparative Superose 6 column (86 cm × 1 cm) and eluted with 0.5 M sodium acetate, pH 7.0, at a flow rate of 4 ml/h. Fractions (1 ml) were collected and assayed for hexuronic acid content by the carbazole procedure of Bitter and Muir [33]. Fractions 34–40 were pooled and concentrated to a final volume of 1 ml in Centricon centrifugal microconcentrators (10000-M_r cut-off; Amicon). The pool was rechromatographed on the same column under identical conditions. Hyaluronate concentrations in the fractions were determined by the carbazole assay with glucuronolactone as standard. Hyaluronate chain lengths were determined by electron microscopy as described below.

Testicular hyaluronidate digestion

Samples of HA_{short} and high-M_r hyaluronate from rooster comb were dissolved at 100 μg/ml in 0.1 M sodium acetate/0.15 M NaCl, pH 5.5. Testicular hyaluronidase (Sigma; 10 μg/mg hyaluronate) was added, and the samples were digested for 6 h at 37 °C. Aliquots of each digest (10–40 μl) were chromatographed on an analytical Sephadex G-50 column (31 cm × 1 cm) which was eluted with 0.5 M sodium acetate, pH 7.0, at a flow rate of 4 ml/h. Fractions (1 ml) were collected and analysed for hexuronic acid content as above. Undigested control samples of hyaluronate were chromatographed on the same column under similar conditions.

Reconstitution of aggregates

Proteoglycan monomers, core protein and link protein from chondrosarcoma tissue, as well as non-reduced and reduced and alkylated hyaluronate-binding-region fragment from bovine nasal cartilage, were dissolved in 4 M GuHCl/0.05 M sodium acetate, pH 5.8, at final concentrations of 1 mg/ml. HA_{short} was dissolved in 0.5 M sodium acetate, pH 7.0, at a concentration of 100 μg/ml. Link-free aggregates were reconstituted by successively mixing HA_{short} with 10-fold molar excesses of proteoglycan monomers, core protein and hyaluronate-binding region. In some experiments HA_{short} was complexed with hyaluronate-binding region at different molar ratios of 1:0.5, 1:1, 1:3 and 1:5 (hyaluronate/G1 fragment respectively). In control experiments HA_{short} was mixed with a 10-fold molar excess of reduced and alkylated hyaluronate-binding region. Molarities were calculated on the assumption that each

binding region interacts with five hyaluronate disaccharides [7]. Link-stabilized aggregates were prepared at HA_{short}/protein ratios of 1:10 by addition of link protein in amounts equimolar to proteoglycan or proteoglycan fragments. Alternatively HA_{short} was mixed with a 10-fold molar excess of link protein in a similar way. In some experiments a two fold molar excess of link protein to binding-region fragment was used.

Electron microscopy

Reconstituted aggregates were dialysed overnight at 4 °C in a flow-through dialysis apparatus designed for small volume (5–50 μl; Biowerk, Basel, Switzerland) against 50 ml of 0.2 M NH_4HCO_3, pH 7.9. The dialysate was continuously removed by pumping fresh 0.2 M NH_4HCO_3 solution into the dialysate chamber. Mixtures of HA_{short} with reduced and alkylated G1 fragment were dialysed in the same way. Samples were then diluted with the same buffer to obtain a final concentration of 50–100 μg/ml. They were prepared for electron microscopy by glycerol spraying/rotary shadowing [27–29].

HA_{short} was dialysed overnight at 4 °C against 0.2 M NH_4HCO_3, pH 7.9, in the dialysis apparatus, diluted with the same buffer to obtain final concentrations of 0.1–0.5 μg/ml, mixed with an equal volume of 80% glycerol and subjected to glycerol spraying/rotary shadowing or mica sandwich squeezing [34]. Alternatively, hyaluronate samples were diluted with 4 M GuHCl to obtain similar final concentrations, squeezed between two freshly cleaved mica pieces and dried in a high vacuum for 30 min, followed by removal of the GuHCl from the mica surface with ethanol. Specimens were subsequently dried in a high vacuum for 1–2 h and rotary-shadowed at a 9° angle with platinum/carbon, followed by carbon coating from above. Evaluation of the data from electron micrographs was as described previously [35]. Statistical analysis of data sets was as described by Armitage [36].

RESULTS

Preparation of hyaluronate with defined chain length (HA_{short})

High-M_r hyaluronate was depolymerized by autoclaving and then fractionated on Superose 6, followed by rechromatography of a narrow cut fraction on the same column. Figures 2(a) and 2(b) show elution profiles of the first and second chromatographic run respectively as monitored by hexuronic acid content. Fraction 34 of the second run, as indicated by an arrow in Figure 2(b), was subsequently called HA_{short} and used in reconstitution experiments. Before these experiments the HA_{short} fraction was analysed for deacetylation which might have occurred during hydrolysis. For this purpose HA_{short} as well as high-M_r hyaluronate control samples were digested with testicular hyaluronidase and then run on an analytical Sephadex G-50 column. For comparison, undigested samples of HA_{short} and high-M_r hyaluronate were run on the same column and eluted in the void volume. Both digested samples were eluted identically in the included volume, indicating that the hyaluronidase had been able to quantitatively digest the hyaluronate, and suggesting that no deacetylation of HA_{short} had occurred (results not shown).

HA_{short} was visualized by electron microscopy after glycerol spraying/rotary metal shadowing of solutions with low hyaluronate concentrations (0.1–0.5 μg/ml) as shown in Figures 3(a) and 3(b). At higher hyaluronate concentrations, various forms of self-associating structures were observed (not shown). At the low concentrations used, no entangling of hyaluronate strands was apparent, as distances of several micrometres were frequently measured between individual molecules. When

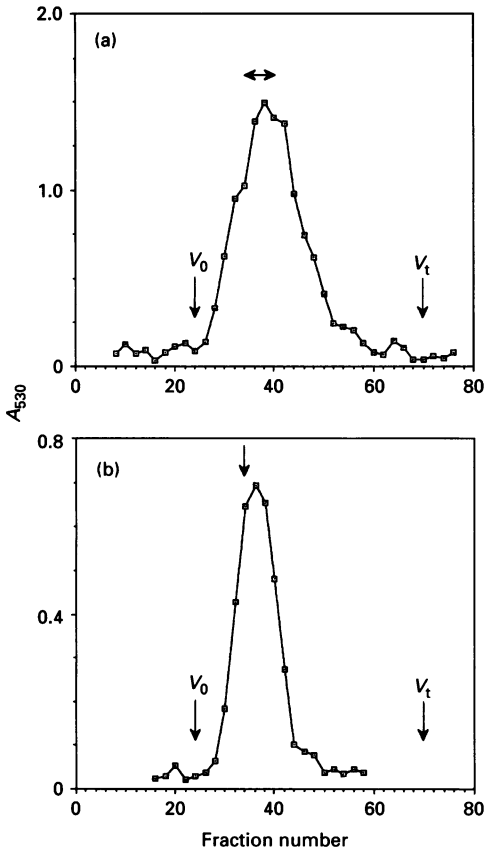

Figure 2 Hexuronic acid elution profiles of hyaluronate after depolymerization by autoclaving

Chromatography on Superose 6 was performed twice. From the first run (**a**) fractions 34–40 were pooled as indicated, concentrated and rechromatographed on the same column (**b**). Material from fraction 34 (HA_{short}; arrow) was used in reconstitution experiments. The excluded (V_0) and total (V_t) volumes of the column are indicated.

sprayed out of 0.2 M NH_4HCO_3, individual hyaluronate strands appeared rather flexible and bent (Figure 3a), but after spraying from 4 M GuHCl and rinsing with ethanol the strands were straight and oriented (Figure 3b). Their length distribution was more narrow with a higher mean length value (460 ± 70 nm; see Figure 5b) than for the molecules sprayed out of NH_4HCO_3 (310 ± 90 nm; see Figure 5a). Similar results were obtained when HA_{short} was prepared for electron microscopy by mica sandwich squeezing out of 0.2 M NH_4HCO_3 (400 ± 80 nm) or 4 M GuHCl (470 ± 60 nm).

Reconstitution of aggregates with HA_{short}

A schematic view of a reconstituted proteoglycan aggregate with all the components mentioned in this work is shown in Figure 1. Addition of suprastoicheiometric amounts of hyaluronate-binding region G1 (Figure 3c), link protein (Figure 3d) or both (Figure 3e) to HA_{short} led to the formation of aggregates. These yielded mainly uninterrupted central filaments with only a few gaps of free hyaluronate, together with a high background of unbound protein molecules. On visual inspection, aggregates with identical central filament structures were observed in similar experiments, when proteoglycan monomers (Figures 4a and 4b) or core protein (Figures 4c and 4d) in the absence (Figures 4a and 4c) or presence (Figures 4b and 4d) of link protein were applied.

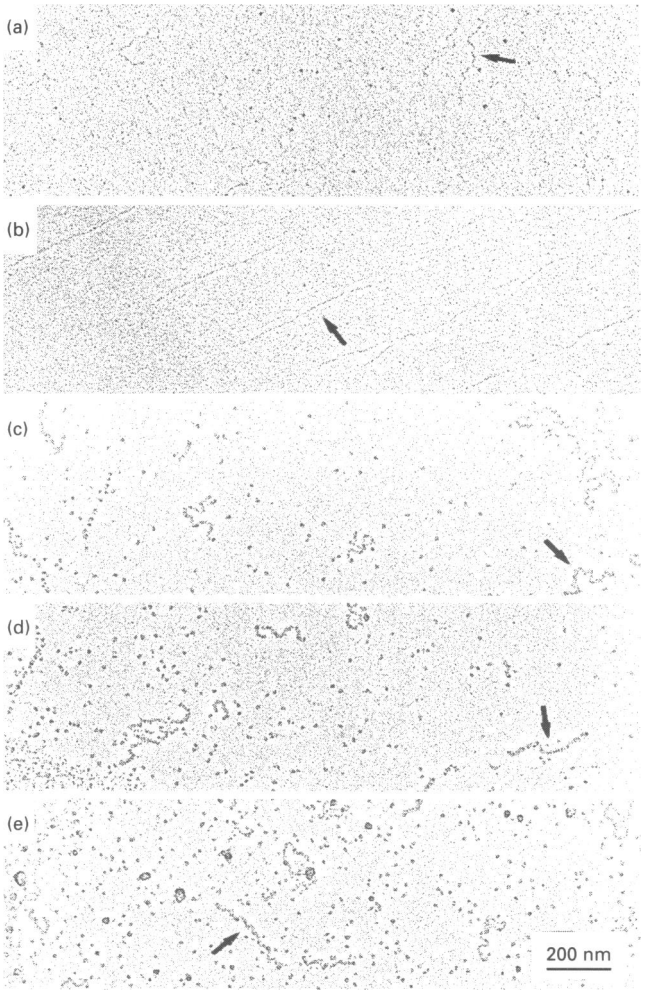

Figure 3 Isolated strands of the HA_{short} and assembly products thereof with G1 and link protein, visualized by electron microscopy after glycerol spraying/rotary shadowing with platinum

Samples were sprayed from 0.2 M NH_4HCO_3 (**a**) or 4 M GuHCl (**b**). The GuHCl-containing specimens were rinsed with ethanol after drying in a high vacuum. In (**a**) no and in (**b**) only very few intermolecular interactions were observed at the low concentrations used. Complexes were formed of HA_{short} with hyaluronate-binding-region fragment G1 (**c**), link protein (**d**) and both G1 and link protein (**e**). The comparison of isolated strands of HA_{short} with complexes thereof clearly visualizes the length change induced by G1 and link protein. Only particles in which no chain entanglement was apparent were measured, as indicated by arrows.

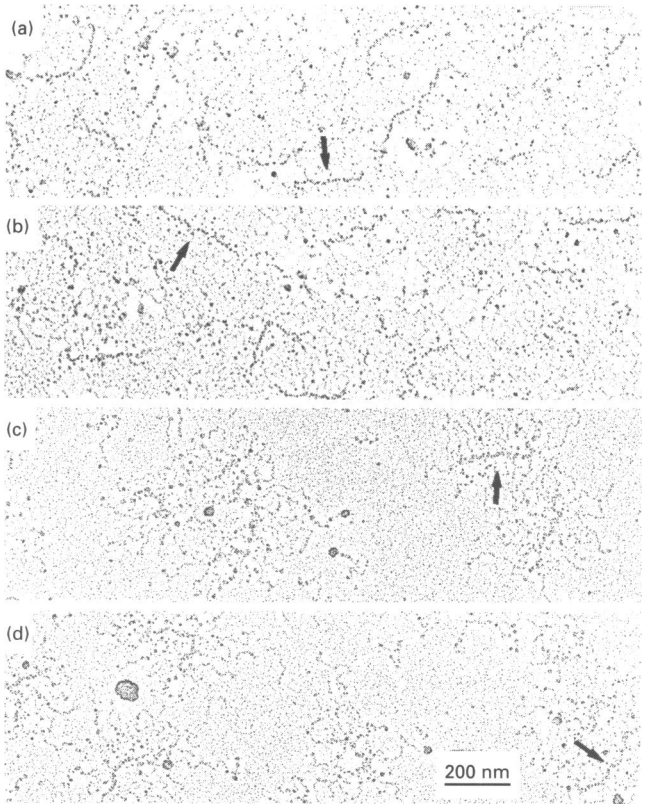

Figure 4 Electron micrographs taken after glycerol spraying/rotary shadowing of reconstituted complexes of HA_{short} with proteoglycan monomers and the core protein

HA_{short} was complexed with intact monomers (**a, b**) and core protein (**c, d**) in the absence (**a, c**) or presence (**b, d**) of link protein. In all cases large suprastoicheiometric amounts of proteoglycan aggregate components were added to the hyaluronate to obtain saturated central filaments. Molarities were calculated on the assumption that each binding region interacts with five hyaluronate disaccharides [7]. Only well-spread-out aggregates were considered for length determination (arrows). The shapes and lengths of link-free and link-stabilized central filaments were similar for all types of aggregate shown.

The lengths of the aggregates formed were compared with either the maximum length of HA_{short}, which we measured in its presumably most extended conformation (460 ± 70 nm) in GuHCl, or the length of HA_{short} sprayed from 0.2 M NH_4HCO_3 (310 ± 90 nm). Binding of hyaluronate-binding-region fragment (G1) or link protein alone to HA_{short} had a profound effect, as the complexes formed were condensed to about half of the length of free hyaluronate sprayed from 4 M GuHCl (Figure 5) or to about 70% of free HA_{short} visualized from 0.2 M NH_4HCO_3. Simultaneous addition of equimolar or suprastoicheiometric amounts of link protein in addition to G1 domain did not cause any detectable further change in the central filament lengths. The length reduction was identical for re-formed aggregates of HA_{short} with aggrecan monomers and fragments in the presence or absence of link protein within error limits (not shown). In control experiments, suprastoicheiometric amounts of reduced and alkylated G1 fragment were added to HA_{short}. No complexes with HA_{short} could be detected (not shown) and consequently no length reduction in HA_{short} was observed, compared with HA_{short} sprayed out of 0.2 M NH_4HCO_3, demonstrating that the shortening of HA_{short} in the aggregate samples is specifically due to the binding of protein. In some experiments, complexes were reconstituted at different degrees of subsaturation by titrating HA_{short} with decreasing amounts of hyaluronate-binding-region fragment. The complexes formed were increasingly longer compared with the fully saturated complexes, showing a dose-dependence of the shortening as fewer and fewer G1 domains were bound to HA_{short} (Figure 6).

These data suggest that the hyaluronate assumes a defined spatial arrangement on binding G1 fragment or the corresponding G1 domain in larger fragments or monomers or link protein alone. Interestingly, at the high molar ratios of binding-region and link protein to hyaluronate, the hyaluronate strands were almost completely saturated and the differences between link-free and heavily stained link-stabilized central filament structure were not as pronounced as seen in earlier experiments which were performed at lower molar ratios of G1 domain to hyaluronate [14]. Control experiments, carried out at equimolar amounts of hyaluronate and binding-region fragment, in the

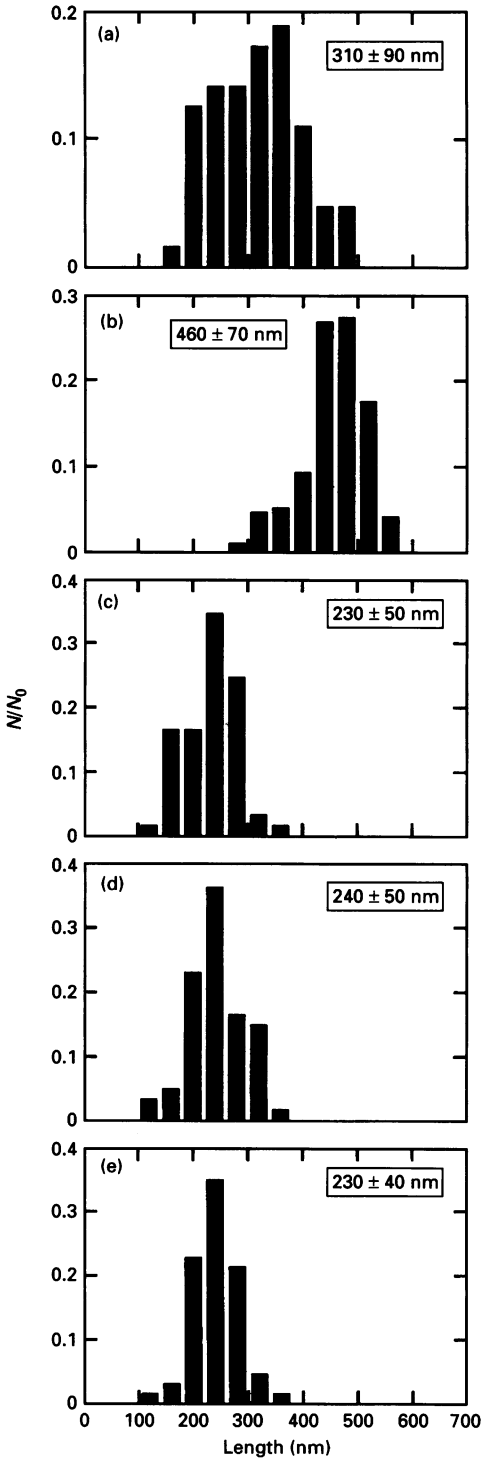

Figure 5 Length distributions of free hyaluronate strands and hyaluronate complexed with hyaluronate-binding-region fragment and/or link protein after glycerol spraying/rotary shadowing

Lengths were measured for isolated strands of HA_{short} from 0.2 M NH_4HCO_3 (**a**) or 4 M GuHCl (**b**), and for complexes of HA_{short} with binding region (**c**), binding region with an equimolar amount of link protein (**d**) or link protein alone (**e**). A total of 100 molecules were measured for each histogram. The length reduction was identical for re-formed aggregates of HA_{short} with aggrecan monomers and fragments in the presence or absence of link protein within error limits. N/N_0 denotes the fraction of molecules with a length within an interval of 40 nm. Mean values and S.D. are given in the diagrams. The differences between (**b**) and (**a**), (**c**), (**d**) or (**e**) were analysed statistically, and values of $P \ll 0.001$ were obtained in all cases.

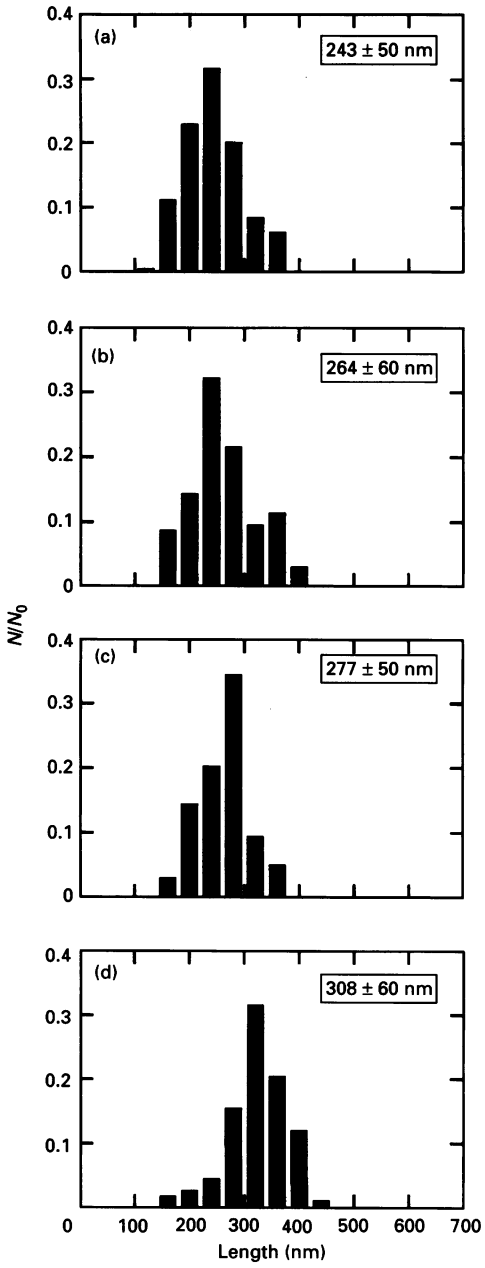

Figure 6 Length distributions of complexes formed by the titration of HA_{short} with hyaluronate-binding-region fragment

Molar ratios of HA_{short}/G1 fragment are 1:5 (**a**), 1:3 (**b**), 1:1 (**c**) and 1:0.5 (**d**). A total of 200 molecules were measured in each experiment. At decreasing amounts of G1 domains complexed to HA_{short}, dose-dependent shortening of the hyaluronate is clearly demonstrated, indicating that this effect is due to each individual ligand. Note that in all cases the length distributions are monodisperse. N/N_0 denotes the fraction of molecules with a length within an interval of 40 nm. Mean values and S.D. are given in the diagrams. The differences between all data sets were tested by statistical analysis. Values of $P < 0.001$ were obtained in all cases, except for (**b**)/(**c**) with $P = 0.02$, and for (**a**)/(**d**) with $P \ll 0.001$.

presence or absence of link protein, clearly demonstrated the densely packed link-stabilized central filament (Figure 7b) compared with the discontinuous link-free central filament (Figure 7a). Thereby it was shown that the link-protein preparation used in reconstitution experiments with HA_{short} was active in forming ternary complexes with hyaluronate and binding region.

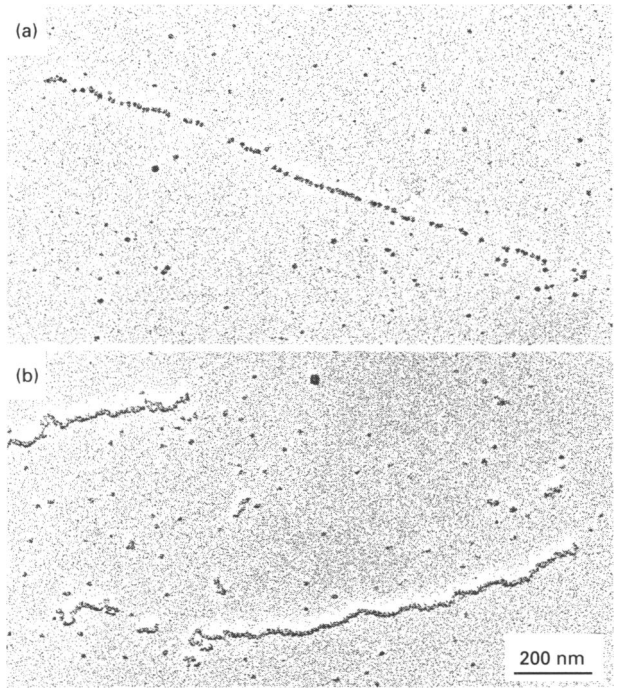

Figure 7 Assembly products formed by the interaction of high-M_r hyaluronate with hyaluronate-binding region without (a) or with (b) link protein after glycerol spraying/rotary shadowing

Equimolar amounts of hyaluronate, quantified as decasaccharide segments, binding-region fragment and link protein were aggregated to show the typical densely packed link-stabilized central filament structure (**b**) which is not obvious under the conditions shown in Figure 5, where the hyaluronate was complexed with suprastoichieometric amounts of ligands. Molarities were calculated as described in Figure 4.

DISCUSSION

In the present study we prepared hyaluronate with narrow chain-length distribution by repeated size-exclusion chromatography of depolymerized high-M_r hyaluronate. Hyaluronate chains of this preparation were visualized by electron microscopy after glycerol spraying/rotary shadowing and exhibited a unimodal chain-length distribution. When proteoglycan monomers or fragments were allowed to bind, the lengths of the central filaments in the aggregates formed were only about half the chain lengths of free hyaluronate which was most extended if sprayed from 4 M GuHCl. The shortening was somewhat less distinct but nevertheless clearly visible for free HA_{short} sprayed from 0.2 M NH_4HCO_3. The interaction of link protein alone with HA_{short} caused the same effect. The ligand-shortening effect could be titrated with decreasing ratios of G1 fragment/hyaluronate in a dose-dependent manner. A shortening of the hyaluronate by half its length means that the observed distance of 12 nm between monomer-binding sites in the central filament [14] corresponds to a stretch of approx. 24 nm of hyaluronate in its fully extended conformation. This equals a repeat of about 24 hyaluronate disaccharide units per 12 nm assuming that the unit per contour length ratio in hyaluronate is the same as determined crystallographically (for references, see [37]). The hyaluronate strand most probably follows a three-dimensional path around parts of individual binding-region or link-protein domains. Reconstituted link-free and link-stabilized aggregates had the same central filament lengths, and simultaneous addition of link protein in even suprastoicheiometric amounts with respect to binding region had no further influence. The binding of one of the central filament components (either the proteoglycan G1 domain or link protein) is sufficient to make the hyaluronate take on the final spatial structure. Apparently link protein does not further contract the central filament, but does probably add molecular mass which gives rise to the heavily stained structure seen in link-stabilized aggregates.

The observation that the length of the central filament is about half of the length of free hyaluronate now explains earlier discrepancies between calculated and totally added hyaluronate in reconstitution studies [14]. In these experiments, hyaluronate contents in aggregates were calculated with a repeat of 12 instead of 24 nm per monomer, and consequently only 50% of added hyaluronate could be accounted for.

It has been reported that hyaluronate strands have the capability of intramolecular self-association even in dilute solutions [38]. On the basis of a combination of viscometric, light-scattering and PAGE examination of hyaluronate with defined chain length, these authors suggested that segments exceeding 40 disaccharide units are capable of intramolecular chain folding in 0.15 M NaCl solutions. Hyaluronate strands in our preparation are considerably longer and should therefore be able to undergo the same folding. This is supported by our observation that HA_{short} samples which were glycerol-sprayed/rotary-shadowed under denaturing conditions (4 M GuHCl) showed longer filaments than samples after preparation from 0.2 M NH_4HCO_3. If intrachain folding occurs in the hyaluronate under the conditions we have used, this would not affect our basic observation of shrinking caused by ligand-binding, but might lead us to underestimate this effect.

Hascall and Heinegård [7] obtained a value of five hyaluronate disaccharide units required as minimum binding site for each hyaluronate-binding region. Our results show that each binding-region domain may strongly attach to a hyaluronate segment of this size, but probably interacts with about 20 more disaccharides on binding by making the hyaluronate take on a defined spatial arrangement within the central filament. This higher value is supported by the value of some eight to ten disaccharides of hyaluronate calculated per core protein at saturation binding [7] and the about 12 disaccharides shown to be required for the formation of the ternary complex hyaluronate–proteoglycan–link protein [39]. Further support is provided by the observation that, during digestion of proteoglycan aggregates from a chondrosarcoma a-A1 preparation with *Streptomyces* hyaluronidase, hyaluronate segments of about 25 disaccharides were protected [40]. Although this is only the length to which the enzyme did not have access, and the minimum length occupied by each binding-region domain actually may be shorter, these results are in reasonable agreement with our present findings. Recent models of G1 and link-protein structures, based on neutron and synchrotron X-ray-scattering data, suggest that the binary complex of these two components should have the dimensions 12 nm × 12 nm [41,42], values that would fit well with our electron-microscopy results.

This study was supported by grants from the Swiss National Science Foundation, the M. E. Müller Foundation, the Swedish Medical Research Council, the Swedish Natural Science Research Council, the Swiss Bundesamt für Bildung und Wissenschaft, the EU within the Human Capital and Mobility Programme (contract no. CHRXCT 930246), the Sandoz Foundation and the Roche Research Foundation.

REFERENCES

1 Heinegård, D. and Paulsson, M. (1984) in Extracellular Matrix Biochemistry (Piez, K. A. and Reddi, A. H., eds.), pp. 277–328, Elsevier Scientific Publications, New York

2 Hardingham, T. E. (1986) in Rheumatology (Kühn, K. and Krieg, T., eds.), vol. 10, pp. 143–183, Karger, Basel
3 Heinegård, D. and Sommarin, Y. (1987) Methods Enzymol. **144**, 319–372
4 Hascall, V. C. (1988) ISI Atlas of Science: Biochemistry, **1**, 189–198
5 Hardingham, T. E. and Muir, H. (1972) Biochim. Biophys. Acta **279**, 401–405
6 Heinegård, D. and Hascall, V. C. (1974) J. Biol. Chem. **249**, 4250–4256
7 Hascall, V. C. and Heinegård, D. (1974) J. Biol. Chem. **249**, 4242–4249
8 Hardingham, T. E. (1979) Biochem. J. **177**, 237–305
9 Tengblad, A. (1981) Biochem. J. **199**, 297–305
10 Franzén, A., Björnsson, S. and Heinegård, D. (1981) Biochem. J. **197**, 669–674
11 Bonnet, F., Dunham, D. G. and Hardingham, T. E. (1985) Biochem. J. **228**, 77–85
12 Wiedemann, H., Paulsson, M., Timpl, R., Engel, J. and Heinegård, D. (1985) Biochem. J. **224**, 331–333
13 Paulsson, M., Mörgelin, M., Wiedemann, H. et al. (1987) Biochem. J. **245**, 763–772
14 Mörgelin, M., Paulsson, M., Hardingham, T. E., Heinegård, D. and Engel, J. (1988) Biochem. J. **253**, 175–185
15 Neame, P. J., Christner, J. E. and Baker, J. R. (1987) J. Biol. Chem. **262**, 17768–17778
16 Doege, K., Fernandez, P., Hassell, J. R., Sasaki, M. and Yamada, Y. (1986) J. Biol. Chem. **261**, 8108–8111
17 Doege, K., Sasaki, M., Horigan, E., Hassell, J. R. and Yamada, Y. (1987) J. Biol. Chem. **262**, 17757–17767
18 Doege, K., Sasaki, M., Kimura, T. and Yamada, Y. (1991) J. Biol. Chem. **266**, 894–902
19 Sai, S., Tanaka, T., Kosher, R. A. and Tanzer, M. L. (1986) Proc. Natl. Acad. Sci. U.S.A. **83**, 5081–5085
20 Oldberg, Å, Antonsson, P. and Heinegård, D. (1987) Biochem. J. **243**, 255–259
21 Fosang, A. J. and Hardingham, T. E. (1989) Biochem. J. **261**, 801–809
22 Mörgelin, M., Heinegård, D., Engel, J. and Paulsson, M. (1994) Biophys. Chem. **50**, 113–128
23 Rosenberg, L., Hellmann, W. and Kleinschmidt, A. (1970) J. Biol. Chem. **245**, 4123–4130
24 Wellauer, P., Wyler, T. and Buddecke, E. (1972) Hoppe Seyler's Z. Physiol. Chem. **353**, 1043–1052
25 Kleinschmidt, A. K. and Zahn, R. K. (1959) Z. Naturforsch, Teil B **146**, 770–779
26 Rosenberg, L., Hellmann, W. and Kleinschmidt, A. (1975) J. Biol. Chem. **250**, 1877–1883
27 Shotton, D. M., Burke, B. and Branton, D. (1979) J. Mol. Biol. **131**, 303–329
28 Fowler, W. A. and Erickson, H. P. (1979) J. Mol. Biol. **134**, 241–249
29 Tyler, J. M. and Branton, D. (1980) J. Ultrastruct. Res. **71**, 95–102
30 Mörgelin, M., Engel, J., Heinegård, D. and Paulsson, M. (1992) J. Biol. Chem. **267**, 14275–14284
31 Heinegård, D. (1977) J. Biol. Chem. **252**, 1980–1989
32 Heinegård, D. and Axelsson, I. (1977) J. Biol. Chem. **252**, 1971–1979
33 Bitter, T. and Muir, H. (1962) Anal. Biochem. **4**, 330–334
34 Mould, P., Holmes, D., Kadler, K. and Chapman, J. (1985) J. Ultrastruct. Res. **91**, 66–76
35 Engel, J. and Furthmayr, H. (1987) Methods Enzymol. **145**, 3–78
36 Armitage, P. (1971) Statistical Methods in Medical Research, Blackwell Scientific Publications, Oxford
37 Arnott, S. and Mitra, A. K. (1984) in Molecular Biophysics of the Extracellular Matrix (Arnott, S., Rees, D. A. and Morris, E. R., eds.), pp. 41–67, Humana Press, New York
38 Turner, R. E., Lin, P. and Cowman, M. K. (1988) Arch. Biochem. Biophys. **265**, 484–495
39 Kimura, J. H., Hardingham, T. E., Hascall, V. C. and Solursh, M. (1979) J. Biol. Chem. **254**, 2600–2609
40 Faltz, L. L., Caputo, C. B., Kimura, J. H., Schrode, J. and Hascall, V. C. (1979) J. Biol. Chem. **254**, 1381–1387
41 Perkins, S. J., Nealis, A. S., Dunham, D. G., Hardingham, T. E. and Muir, H. (1991) Biochemistry **30**, 10708–10716
42 Perkins, S. J., Nealis, A. S., Dunham, D. G., Hardingham, T. E. and Muir, H. (1992) Biochem. J. **285**, 263–268

Received 22 July 1994/5 December 1994; accepted 12 December 1994